RESPONSE OF CLAY AND CLAY SHALE TO HEAVY DYNAMIC LOADING

L. V. Al'tshuler and M. N. Pavlovskii

Results are presented on the dynamic compressibility of several types of rock. Shock compression curves have been recorded up to 500 kbar for four types of clay and a shale, together with the initial parts of the expansion isentropes. The curves have features related to phase transitions, and conclusions are drawn on the applicability of adiabatic addition to these systems.

1. Shock Compressibility. We examined: A) nearly white surface clays with two different water contents; B) green deep-lying clay with the same water contents; C) clay shale. Elemental and x-ray structural analyses showed that the main component in each case was silica, which in the green clay and shale was accompanied by minerals of kaolinite type. A_4 and B_4 denote water contents W of 4% by weight, while A_{20} and B_{20} denote 20%, etc.

The shock compressibility was measured by reflection [1, 2]. The wave velocity was measured by an electrical contact method [1]. The specimens had thicknesses of 4-6 mm. We used dynamic adiabatic compression curves for iron and aluminum [3] in making the necessary constructions in the plot of pressure against mass velocity. The expansion isentropes for the screens adjoining the specimen were identified [2] with mirror images of shock adiabatics.

Table 1 gives the results, where the symbols are as follows: ρ_0 is the initial density (g/cm^3); U_S is the mass velocity (km/sec) of the shield material (usually aluminum) (U_S is primed when the material was copper); D is the wave velocity (km/sec); U is the mass velocity (km/sec) behind the shock front in the specimen; P (kbar) is the shock pressure; ρ is the density (g/cm^3) of the compressed material; and V (cm^3/g) is the specific volume.

Figure 1 shows the results of Table 1 in D and U coordinates, where curves 1 and 2 are for A_{20} and A_4, while 3 and 4 are for B_{20} and B_4, and 5 is for the shale.

The following equations describe satisfactorily the observations for the clays:

$$D\,(A_{20}) = 3.05 + 1.23\,U,\quad D\,(A_4) = 2.78 + 1.21\,U$$
$$D\,(B_{20}) = 2.20 + 1.50\,U,\quad D\,(B_4) = 1.60 + 1.47\,U$$

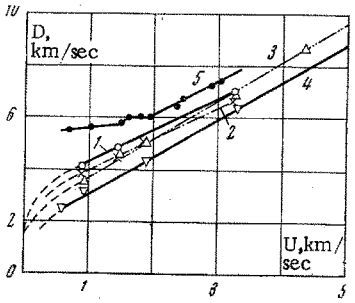

Fig. 1

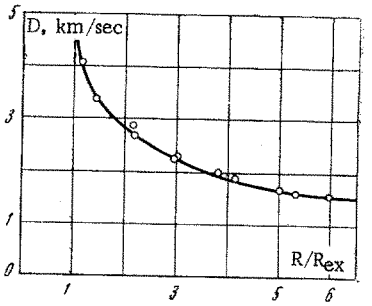

Fig. 2

Moscow. Translated from Zhurnal Prikladnoi Mekhaniki i Tekhnicheskoi Fiziki, No. 1, pp. 171-176, January-February, 1971. Original article submitted December 15, 1969.

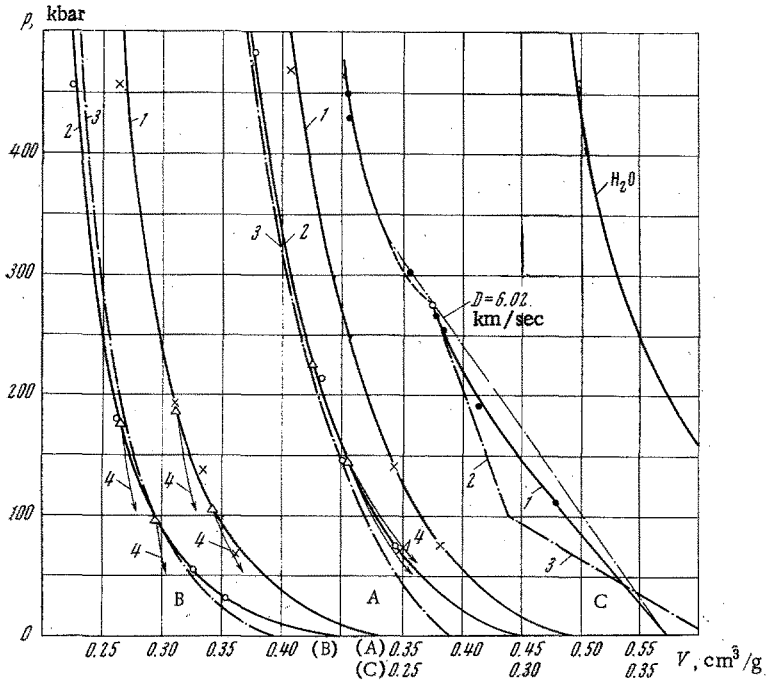

Fig. 3

TABLE 1

Material	ρ_0, g/cm³	U_s, km/sec	D, km/sec	U, km/sec	P, kbar	ρ/ρ_0	ρ, g/cm³	V, cm³/g
A_{20}	2.03	0.69	4.12	0.91	76.5	1.284	2.62	0.382
	2.03	1.14	4.83	1.45	142.5	1.428	2.91	0.344
	2.06	2.70	7.02	3.26	471	1.868	3.85	0.260
A_4	2.23	0.69	3.85	0.89	77	1.307	2.91	0.344
	2.24	1.14	4.46	1.44	145	1.475	3.30	0.302
	2.27	1.50	5.15	1.84	215	1.556	3.54	0.283
	2.24	2.70	6.70	3.23	485	1.933	4.33	0.231
B_{20}	2.02	0.69	3.55	0.95	68	1.364	2.76	0.362
	2.04	1.14	4.63	1.47	139	1.466	2.99	0.335
	2.02	1.50	5.10	1.90	194	1.594	3.22	0.311
	2.00	2.70	6.97	3.28	458	1.892	3.79	0.264
	2.02	3.70	8.70	4.37	770	2.010	4.06	0.246
B_4	2.15	0.35′	2.52	0.605	32.8	1.316	2.83	0.353
		0.69	3.20	0.96	66	1.429	3.07	0.326
		1.50	4.39	1.90	179	1.763	3.80	0.263
		2.70	6.40	3.32	457	2.075	4.46	0.224
C	2.77	0.69	5.53	0.72	111	1.150	3.19	0.313
		1.14	5.62	1.23	191	1.280	3.55	0.282
		1.43	5.80	1.51	243	1.352	3.75	0.267
		1.50	6.00	1.61	268	1.369	3.79	0.264
		1.68	6.06	1.81	304	1.427	3.95	0.253
		1.80	6.05	1.98	332	1.486	4.12	0.243
		1.64′	6.43	2.38	424	1.589	4.40	0.227
		1.71′	6.78	2.46	462	1.570	4.35	0.230
		2.72	7.29	2.91	590	1.664	4.62	0.217

For A_{20} we also determined the effects of R (distance from the center) on the speed of the divergent shock wave produced by a small spherical explosive charge (diameter 50 mm) composed of a TNT–hexogene mixture (Fig. 2).

The shock-wave speed and path were determined via sets of contacts within the clay at various distances from the charge. We found that the speed of the degenerate shock wave in moist clay was almost equal to that of sound in water.

Figure 2 provided an approximate form for the initial part of the D–U relation for A_{20}. An analogous initial part was assumed for B_{20}. The shale differed in that the shock-compression curve consisted of

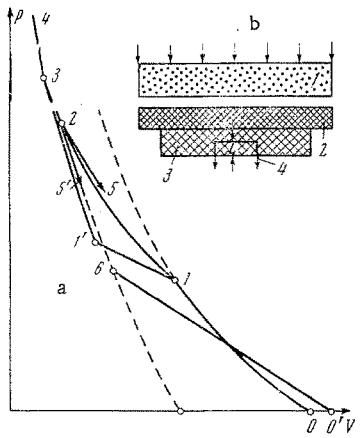

Fig. 4

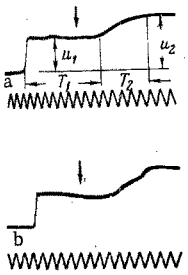

Fig. 5

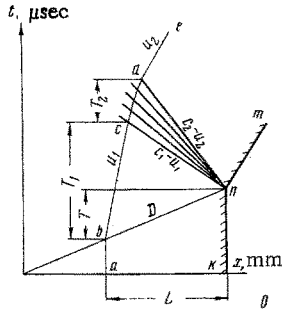

Fig. 6

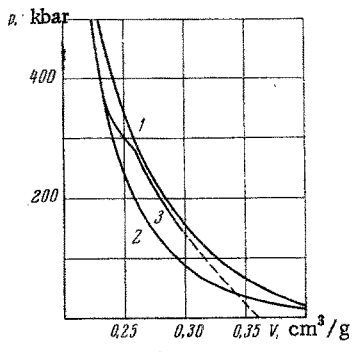

Fig. 7

several parts, which were clearly seen in the D−U relation (Fig. 1). The first part is a slightly sloping line that resembles the initial D−U relation for graphite in transition to diamond [4]. There is a short range near 280 kbar where the wave speeds increase rapidly, which is followed by a horizontal part representing a first-order phase transition. The upper branch relates to the high-pressure phase. It is convenient to interpret the results in P−V coordinates, and Fig. 3 shows the results for the shale and the four clay specimens.

The observed shock adiabatics are the solid lines 1 and 2. The adiabatic for shale has two branches, which relate to the low- and high-pressure phases. The curves for the clays are monotonic and are nearly parallel above 100 kbar.

2. Structure of the Rarefaction Waves. A shale or clay is a composite mineral system that may have many phase transitions. If the transition times are finite and comparable with the recording time, the shock-compression curves represent a set of nonequilibrium states with variable phase compositions. The observed curves may remain monotonic and may differ little in shape from the adiabatics for homogeneous stable media (Fig. 4a). The actual state can be deduced from observations on rarefaction waves. The maximum speed C of such a wave is related to the slope of the isentropic expansion curve by

$$V^2\left(\frac{\partial P}{\partial V}\right)_S = C^2 \qquad (2.1)$$

If there are no phase transformations (curve 01234 is the adiabatic for a homogeneous medium), the slope of the isentrope will be less than that of the dynamic adiabatic (expansion along line 2-5). If the medium contains considerable amounts of the denser phase along with the initial phase, the expansion will occur along 2-5'. Additional evidence for phase transformations comes from rarefaction shock waves [5-7], with a stepwise return to the initial phase (6-0' transition) at the front.

The strength may affect the interpretation of the results [1, 8]. A medium with an appreciable yield point has elastic deformation during the initial expansion, and the elastic-expansion wave has $C_e > C$. In the general case it is very difficult to distinguish an elastoplastic expansion curve from the recovery curve for a heterogeneous medium.

A magnetic method [1, 7, 9] was used to record the shapes of the compression and expansion shock waves. Figure 4b shows the results, while Fig. 5 shows typical oscillograms (a for clay, b for shale). The π-shaped transducers 4 were made of aluminum foil and were placed at a depth L ≈ 6 mm in the specimen 3 (1 is the explosive and 2 is the shield).

The first deflection corresponds to arrival of the pressure wave at the transducer. After this wave has reached the free surface (knm is the path taken by the surface), a centered tension wave propagates within the specimen (x−t diagram in Fig. 6). The second kick corresponds to arrival of this wave at the transducer after time T_1 (abcde is the path taken by the transducer), while T_2 corresponds to the dispersion of the tension wave. Then T_1, U_1, and the known L and D give the maximum velocities behind the shock-wave front. The x−t diagram of Fig. 6 shows that

TABLE 2

№	Material	ρ_0, $\frac{g}{cm^3}$	P, kbar	D, $\frac{km}{sec}$	U, $\frac{km}{sec}$	$\frac{\rho}{\rho_0}$	ρ, $\frac{g}{cm^3}$	V, $\frac{cm^3}{g}$	C, $\frac{km}{sec}$
1	B_4	2.15	99	3.51	1.31	1.594	3.43	0.292	7.17
2			178	4.38	1.89	1.760	3.79	0.264	6.79
3	B_{20}	2.03	107	4.16	1.27	1.440	2.92	0.343	5.61
4			188.5	5.02	1.85	1.583	3.21	0.311	7.60
5	A_4	2.25	146.6	4.52	1.44	1.470	3.30	0.303	4.90
6			227	5.14	1.96	1.616	3.64	0.275	4.87
7	C	2.77	276	6.00	1.64	1.378	3.82	0.262	6.3

TABLE 3

P, kbar	V, cm^2/g				
	H_2O measured	Dry fraction of clay A, calc.	Dry fraction of clay B, calc.	Hygroscopic clay A_4, calc.	Hygroscopic clay B_4, calc.
0	1.000	0.363	0.369	0.388	0.394
30	0.724	0.344	0.329	0.359	0.345
60	0.658	0.327	0.304	0.340	0.318
100	0.600	0.307	0.281	0.318	0.294
150	0.557	0.286	0.264	0.297	0.276
200	0.525	0.269	0.254	0.279	0.264
250	0.500	0.256	0.245	0.266	0.255
300	0.482	0.246	0.238	0.255	0.248
350	0.467	0.236	0.233	0.245	0.243
400	0.455	0.227	0.229	0.237	0.238
450	0.445	0.220	0.225	0.230	0.234
500	0.436	0.215	0.222	0.223	0.231

$$C = U_1 + \frac{L - U_1 T_1}{T_1 - L/D} \tag{2.2}$$

Table 2 gives the results for the negative-pressure waves for materials C, B_4, B_{20}, and A_4. The arrows in the oscillograms indicate the calculated instants for initiation of the tension waves when the shock waves reach the free surface, which are separated by T = L/D from the instant of the first kick.

Arrows 4 in Fig. 3 show the most likely positions for the initial parts of the isentropes. Dry white clay (A in Fig. 3) had an isentrope slope close to that of the shock-compression adiabatic, which implies that there were no nonequilibrium heterogeneous states, at least in the range covered (100-230 kbar), and also that strength effects were negligible.

The green clay (dry or moist) showed a different picture (Fig. 3B), as the negative-pressure curves are much steeper than the shock adiabatics, and their position indicates that there were denser and less compressible components.

Figure 5b and many similar results show that shale gives a complicated structure in the negative-pressure waves, which contain shock-rarefaction waves at the end of the expansion. Figure 3C shows qualitatively the corresponding shape of the expansion curve in the P–V diagram. This curve has a steeply falling section (dot-and-dash curve 2) representing the compressibility of the dense phases and a transition (dot-and-dash line 3) arising when these decompose. There is a pronounced hysteresis loop in the loading-unloading cycle.

3. Discussion. Each clay contained a solid phase and a liquid one. We neglect the inhomogeneity of the solid phase and consider the clay as a two-component system (water plus a dry component).

The additive approximation [10] gives the volume of the shock-compressed mixture as the sum of the volumes of the components as attained by individual compression in the monolithic state.

Let α be the proportion of water by weight, $V^\circ(P)$ the specific volume of water at pressure P, and V_c the specific volume of the dry fraction; then the volume of the mixture is

$$V(P) = \alpha V^{\circ}(P) + (1 - \alpha) V_{c}(P) \qquad (3.1)$$

The shock-wave adiabatic for water is known [11, 12] and the second column in Table 3 gives the specific volume as a function of pressure. The next column gives V_c as deduced from the shock adiabatics for A_{20} and water via (3.1). This equation was also used to derive the shock adiabatic for A_4 (curve 3 in Fig. 3A), which shows good agreement between the observed and additive adiabatics at pressures above 120 kbar but an appreciable discrepancy that increases toward lower P, which we ascribe to porosity in the dry clay. Quite high pressures are needed to close the micropores completely, since the volume of these is still 2.5% of the total volume even at 100 kbar.

Figure 3B (green clay) gives similar results, though here the pressure for zero porosity is about 60 kbar. The most important result for shale is that there are clearly phase transitions at the pressures representing the first part of the shock-wave adiabatic.

Figure 7 compares the results for the shale and dry clays. At about 200 kbar the compressibility of green clay (curve 2) substantially exceeds that of white (curve 1) on account of phase transitions, but the two curves come together at higher pressures. Curve 3 is for shale, which is highly porous in the initial state, and it approaches the curve for white clay at about 140 kbar. The phase transition at 280 kbar makes the shale curve almost the same as the green-clay one. The three curves are virtually indistinguishable above 500 kbar, which reflects the common trend in the compression of silicates and aluminosilicates, which at high pressures give close-packed arrays of oxygen ions that are very similar in compressibility and specific volume.

LITERATURE CITED

1. L. V. Al'tshuler, "Use of shock waves in high-pressure physics," Usp. Fiz. Nauk, 85, No. 2, 197 (1965).
2. L. V. Al'tshuler, M. N. Pavlovskii, L. V. Kuleshova, and G. V. Simakov, "Shock compression of alkali halides at high pressures and temperatures," Fiz. Tverd. Tela, 5, No. 1, 279 (1963).
3. L. V. Al'tshuler, S. B. Kormer, A. A. Bakanova, and R. F. Trunin, "The equations of state for aluminum, copper, and lead at high pressures," Zh. Éksp. Teor. Fiz., 38, No. 3, 790 (1960).
4. M. N. Pavlovskii and V. P. Drakin, "The metallic form of carbon," Zh. Éksp. Teor. Fiz., Pisma v Red., 4, No. 5 (1966).
5. Ya. B. Zel'dovich and Yu. P. Raizer, Physics of Shock Waves and High-Temperature Hydrodynamic Phenomena [in Russian], Moscow, Fizmatgiz (1963).
6. A. G. Ivanov and S. A. Novikov, "Negative-pressure shock waves in iron and steel," Zh. Éksp. Teor. Fiz., 40, No. 6, 1880 (1961).
7. L. V. Al'tshuler, M. N. Pavlovskii, and V. P. Drakin, "Phase transitions in compression and tension shock waves," Zh. Éksp. Teor. Fiz., 52, No. 2, 400 (1967).
8. L. V. Al'tshuler, S. B. Kormer, M. I. Brazhnik, L. A. Vladimirov, M. P. Speranskaya, and A. I. Funtikov, "The high-pressure isentropic compressibilities of aluminum, copper, and lead," Zh. Éksp. Teor. Fiz., 38, No. 4, 1061 (1960).
9. M. N. Pavlovskii, "Production of metallic modifications of germanium and silicon under conditions of shock compression," Fiz. Tverd. Tela, 9, No. 11, 3192 (1967).
10. A. N. Dremin and I. A. Karpukhin, "A method of determining the shock-wave adiabats of finely divided materials," Zh. Prikl. Mekhan. i Tekh. Fiz., No. 3 (1960).
11. J. M. Walsh and M. H. Rice, "Equation of state of water to 250 kilobars," J. Chem. Phys., 26, No. 4, 824-830 (1957).
12. L. V. Al'tshuler, A. A. Bakanova, and R. F. Trunin, "Phase transitions in the compression of water by strong shock waves," Dokl. Akad. Nauk SSSR, 121, No. 1, 67 (1958).